

Probing the Kinetics of Membrane-Mediated Helix Folding

Matthew J. Tucker,[†] Jia Tang,[†] and Feng Gai*

Department of Chemistry, University of Pennsylvania, Philadelphia, Pennsylvania 19104

Received: February 11, 2006; In Final Form: March 9, 2006

The kinetics of peptide–membrane association have been studied previously using stopped-flow tryptophan fluorescence; however, such experiments do not directly report the coil-to-helix transition process, which is a hallmark of peptide–membrane interaction. Herein, we report a new method for directly assessing the kinetics of the helix formation accompanied by the peptide–membrane association. This method is based on the technique of fluorescence resonance energy transfer (FRET) and an amino acid FRET pair, *p*-cyano-L-phenylalanine and tryptophan. To demonstrate the utility of this method, we have studied the membrane-mediated helix folding dynamics of a mutant of magainin 2, an antibiotic peptide found in the skin of the African clawed frog, *Xenopus laevis*. Our results indicate that the coil-to-helix transition occurs during the binding of the peptide to the lipid vesicle (1-palmitoyl-2-oleoyl-*sn*-glycero-3-phosphocholine/1-palmitoyl-2-oleoyl-*sn*-glycero-3-[phospho-*rac*-(1-glycerol)], 3:1, wt/wt) but prior to the full insertion of the peptide into the hydrophobic region of the lipid bilayers.

Introduction

Peptide–membrane interactions play a crucial role in many biological processes,^{1–3} such as membrane lysis, fertilization, and viral infection. Therefore, it has attracted considerable interest in the past. While there have been a plethora of studies devoted to the understanding of the backbone conformation, orientation, membrane environment, depth of insertion, and thermodynamics of membrane-bound peptides,^{4–11} there have been relatively fewer studies on the kinetics of peptide–membrane association. Hence, a truly quantitative description of the molecular mechanism of peptide–membrane interactions remains an important goal.

Many membrane-binding peptides, such as antimicrobial peptides, are amphipathic and, therefore, often adopt random conformations in aqueous solution but fold into α -helical structures when associated with lipid bilayers. Thus, the coil-to-helix transition is a hallmark of peptide–membrane association. However, for most of the membrane-binding peptides studied in the past it is not clear when and where such transition takes place, due to the lack of a suitable experimental approach that can directly monitor the formation of the helix. One model suggests that the helix formation is associated with the process of binding and occurs at the interfacial region of the lipid bilayers,^{7,12–17} which is followed by insertion, whereas a different view suggests that the coil-to-helix transition occurs only after the peptide is inserted.^{18,19} Recently, stopped-flow tryptophan (Trp) fluorescence as well as fluorescence resonance energy transfer (FRET) from the Trp to lipid-bound probes have been employed to study the kinetics of membrane association of several peptides and have provided many insights into our understanding of the mechanism of peptide–membrane interaction,^{18,20–23} including pore formation. However, these techniques do not allow the direct observation of the coil-to-helix transition process. In principle, the kinetics of protein secondary

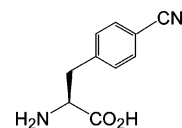


Figure 1. Structure of *p*-cyano-L-phenylalanine.

structure formation upon membrane association can be examined by stopped-flow circular dichroism (CD) spectroscopy.^{18,24,25} Nonetheless, stopped-flow CD has not been broadly used in peptide–membrane binding studies because of its relatively low sensitivity and, thus, the large quantity of peptide sample required, especially for smaller peptides.^{18,26} Therefore, it would be quite advantageous to develop a sensitive and easy-to-use method for directly assessing the kinetics of the helix formation in the process of peptide–membrane association. Here, we introduce such a method that is based on the technique of fluorescence resonance energy transfer.

The FRET technique, which relies on the fact that the efficiency of energy transfer from the donor to the acceptor is distance-dependent, is commonly used in protein and peptide conformational studies.^{27,28} Herein, we aimed to use FRET in conjunction with the stopped-flow technique to study the membrane-mediated helix folding dynamics of amphipathic peptides. In many FRET studies, a pair of dye molecules is often employed to serve as the FRET pair. However, using a FRET dye pair in membrane-binding studies could be problematic because most fluorescent dye molecules are bulky and hydrophobic. Thus, it can significantly affect the properties of the membrane-binding peptides of interest. To minimize any structural perturbations caused by introducing a FRET pair into the native peptide sequence, we propose to use a new FRET pair, *p*-cyano-L-phenylalanine (Phe_{CN}) and Trp, in conjunction with stopped-flow fluorescence, to probe the membrane-mediated helix folding dynamics.

Recently, we have shown Phe_{CN} (Figure 1) is an efficient FRET donor to Trp with a Förster distance of about 16 Å, which has been used to study the conformational distribution of unstructured peptides²⁹ and also the thermally and urea-induced

* Author to whom correspondence should be addressed. E-mail: gai@sas.upenn.edu.

[†] These authors contributed equally to this work.

unfolding transitions of a 16-residue β -hairpin.³⁰ The Phe_{CN}–Trp FRET pair offers several advantages over dye molecules in the study of peptide–membrane interactions because (a) Phe_{CN} is a non-natural amino acid, which may be regarded as a derivative of either Phe or Tyr, and therefore can be easily placed in particular regions of a polypeptide chain by standard peptide synthesis methods, (b) mutation of a native residue with Phe_{CN} should cause only a minimal perturbation to the native conformation, owing to its small size, (c) the nitrile group has a polarity between that of an amide group and a methylene, so Phe_{CN} should be readily accommodated either in the hydrophobic interior or on the hydrophilic surface of a membrane, (d) there is no need for further incorporation of Trp into the peptide of interest if the native sequence already contains a Trp residue, which is quite common in membrane-binding peptides, and (e) the Trp fluorescence may also be used to monitor the process of insertion and association.

To demonstrate the utility of this method, we studied the membrane-mediated folding kinetics of an analogue of magainin 2. Magainin 2 is an antimicrobial peptide isolated from the skin of the African clawed frog, *Xenopus laevis*¹ and consists of 23 amino acids with the following sequence: GIGKFLHSAKKF-GKAFVGQIMNS. It has been shown by NMR and CD spectroscopies that magainin 2 adopts a random conformation in aqueous solution but an α -helical structure when bound to lipid vesicles.^{9,31} Depending on the experimental conditions, however, the final conformation could be a monomeric helix, a helical dimer, or even a pore-forming supracomplex.^{5,13,15,20,32–35} To use the FRET method discussed above, we added a Phe_{CN} residue to the N-terminus of a magainin 2 mutant, i.e., F12W,³⁶ and the resultant sequence is Phe_{CN}-GIGKFLHSAKK-W-GKAFVGQIMNS (magainin-2-P1).

Experimental Section

Materials. Magainin-2-P1 was synthesized using the standard Fmoc-based solid-phase method on a peptide synthesizer (PS3, Protein Technologies, Inc., MA), purified by reverse-phase high-performance liquid chromatography, and verified by mass spectrometry. All peptide solutions were prepared by directly dissolving the lyophilized solids in 50 mM (CD and static fluorescence) or 100 mM (stopped-flow) sodium phosphate buffers (pH 7.0). The final concentration was determined optically using the Trp absorbance at 280 nm ($\epsilon_{280} = 6440 \text{ M}^{-1} \text{ cm}^{-1}$). 1-Palmitoyl-2-oleoyl-*sn*-glycero-3-phosphocholine (POPC) and 1-palmitoyl-2-oleoyl-*sn*-glycero-3-[phospho-*rac*-(1-glycerol)] (sodium salt) (POPG) were purchased from Avanti Polar Lipids (Alabaster, AL). All vesicle solutions were prepared using 100 mM sodium phosphate buffer (pH 7.0).

Vesicle Preparation. A mixture of POPC/POPG (3:1, wt/wt) with a total concentration of 2 mg/mL was prepared in 100 mM phosphate buffer (pH 7.0). This mixture was then taken through a freeze–thaw–vortex process. After this process was repeated five times, the vesicle suspension was extruded through a polycarbonate membrane filter with pore diameters of 200 nm by an extruder (Avanti Polar Lipids).

CD Measurements. The far-UV CD spectra at 25 °C were collected on an AVIV 62DS spectropolarimeter (Aviv Associates, NJ) using a 1 mm quartz cell. The peptide concentration was 30 μM , and the vesicle concentration was 1 mg/mL of POPC/POPG (3:1, wt/wt). Mean residue ellipticity was calculated using the equation $[\theta] = (\theta_{\text{obs}}/10lc)/N$, where θ_{obs} is the ellipticity in millidegrees, l is the optical path length (cm), c is the concentration of the peptide (M), and N is the number of residues.

Absorption Measurements. All UV–vis spectra were measured on a Lambda 25 UV–vis spectrometer (Perkin-Elmer, MA).

Fluorescence Measurements. The fluorescence spectra were collected on a Fluorolog 3.10 spectrofluorometer (Jobin Yvon Horiba, NJ) using a 1 cm quartz sample holder. The spectral resolution was 2 nm (for both excitation and emission). Temperature was controlled at 25 °C using a TLC 50 Peltier temperature controller (Quantum Northwest, WA). The peptide concentration was 25 μM , and the vesicle concentration was approximately 0.6 mg/mL of POPC/POPG (3:1, wt/wt).

Stopped-Flow Fluorescence Apparatus. The stopped-flow fluorescence kinetics were measured using a SFM-300 stopped-flow module (Bio-logic, Claix, France) equipped with home-built optics. The excitation light was derived from a Fluorolog 3.10 spectrofluorometer and was coupled to the observation head of the stopped-flow unit through a multimode optical fiber bundle (77539, Newport Corporation, CT). Fluorescence was collected perpendicular to the excitation beam using a similar optical fiber bundle (77577) and was detected by a Hamamatsu R928P photomultiplier (Hamamatsu Photonic K. K., Hamamatsu, Japan). Current amplification was achieved by a SR750 current amplifier (Stanford Research Systems, TX), and voltage digitization was carried out by a CS1602 Gagescope (Gage Applied, Canada). In experiments (i.e., Figures 4 and 5) where the Trp fluorescence was monitored, a long-pass filter with a cut-on wavelength of 315 nm (Edmund Industrial Optics, NJ) was used to eliminate the excitation light and also the donor fluorescence, whereas in experiments where the Phe_{CN} fluorescence was employed as the probe (i.e., Figure 6), a UV band-pass filter centered at 299 nm with a bandwidth of 22 nm (300FS25-12.5, Andover, NH) was used. For the stopped-flow experiments shown here, a microcuvette $\mu\text{FC-08}$ with a path length of 0.8 mm was used. The dead time of the current system was determined to be ~ 1 ms (data not shown) by measuring the quenching of *N*-acetyl-tryptophanamide (NATA) fluorescence by *N*-bromo-succinamide (NBS).²⁶ The influence of the existence of vesicles on the dead time was also taken into account by pumping the vesicle solution from the third syringe into the observation head simultaneously with NATA and NBS. For the peptide–vesicle association experiments, the reaction was initiated by mixing equal volumes of the peptide solution with the vesicle solution described above. The final peptide concentration was 40 μM , and the temperature was controlled at 25 °C. Under these conditions, the absorbance of the peptide sample was approximately 0.6 at 240 nm and 0.2 at 290 nm, respectively. The stopped-flow traces shown below correspond to an average of 6–10 shots.

Results and Discussion

Static CD and Fluorescence Studies. Matsuzaki et al. have shown that F12W of magainin 2 exhibits similar membrane binding properties as the wild type.³⁶ Consistent with their results, the far-UV CD spectra of magainin-2-P1 show that it is unfolded in aqueous solution but folds into an α -helical conformation when POPC/POPG (3:1, wt/wt) vesicles are present, as indicated by the distinct double minima at 208 and 222 nm in its CD spectrum (Figure 2). Corroborating these observations, the Trp fluorescence of magainin-2-P1, obtained with an excitation wavelength of 290 nm, increases and shifts to a lower wavelength in the vesicle solution as compared to the fluorescence spectrum of the peptide in a phosphate buffer solution (Figure 3a). Taken together, these results indicate that magainin-2-P1 not only binds to phospholipid vesicles but also forms an α -helix upon membrane association.

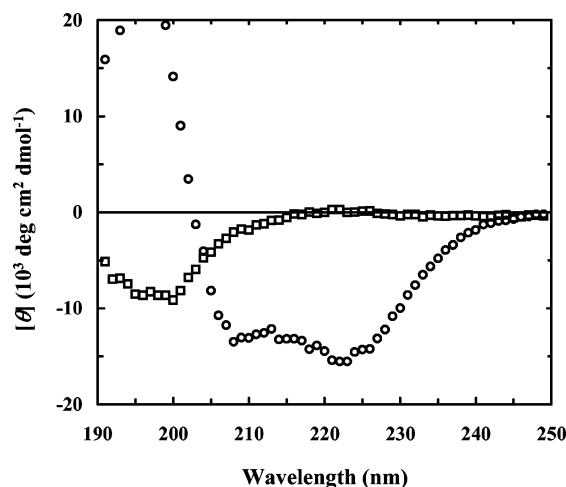


Figure 2. CD spectra of magainin-2-P1 in 50 mM phosphate buffer (pH 7.0) (square) and in POPC/POPG (3:1, wt/wt) vesicle solution (pH 7.0) (circle).

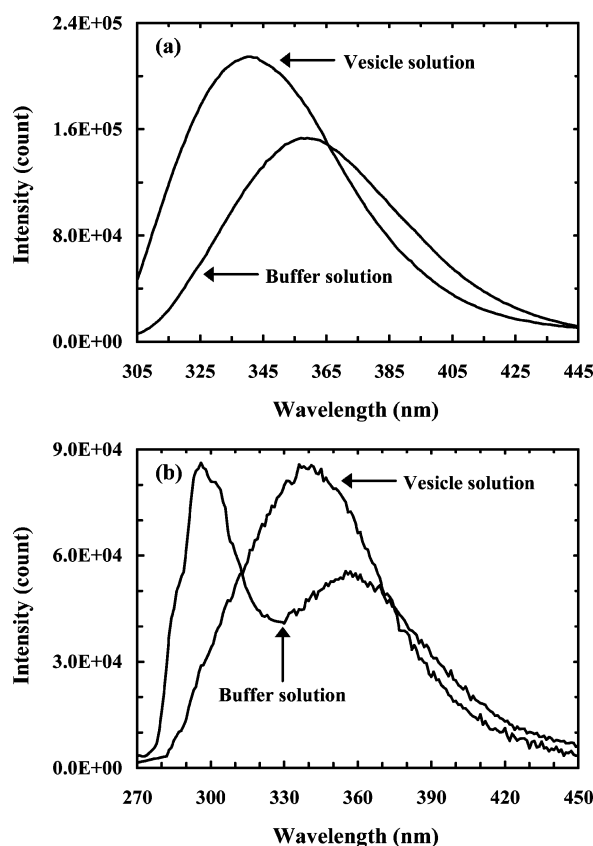


Figure 3. Fluorescence spectra of magainin-2-P1 in phosphate buffer and vesicle solutions: (a) $\lambda_{\text{ex}} = 290$ nm, (b) $\lambda_{\text{ex}} = 240$ nm.

Moreover, when an excitation wavelength of 240 nm was used, where the absorption cross section of Phe_{CN} overwhelms that of Trp and other amino acid chromophores,^{29,30} the resulting emission spectrum of magainin-2-P1 in the buffer solution shows characteristics of FRET (Figure 3b). Nonetheless, the donor fluorescence (i.e., the band at ~295 nm) is still very intense under these conditions, indicating that the peptide adopts a conformational ensemble wherein the Phe_{CN} is relatively distant from the Trp. Therefore, this is in agreement with the CD results and is also consistent with the notion that magainin 2 is intrinsically unfolded in aqueous solution.^{6,9,31} On the contrary, interactions between the peptide and the lipid vesicles result in a significant loss of the donor emission (Figure 3b), indicating

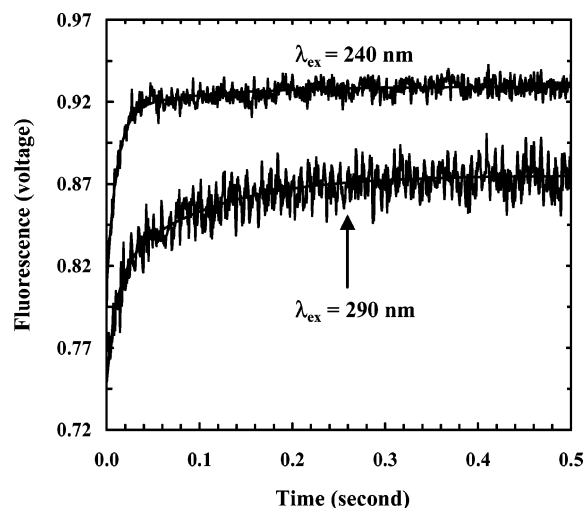


Figure 4. Stopped-flow fluorescence traces obtained with a 315 nm long-pass filter and also different excitation wavelengths, as indicated. Smooth lines are global fits to the following equation, $S(t) = A - B_1 \exp(-t/\tau_1) - B_2 \exp(-t/\tau_2)$, with $\tau_1 = 11$ ms and $\tau_2 = 99$ ms, respectively. For $\lambda_{\text{ex}} = 240$ nm, $A = 0.929$, $B_1 = 0.109$, and $B_2 = 0.014$; for $\lambda_{\text{ex}} = 290$ nm, $A = 0.875$, $B_1 = 0.067$, and $B_2 = 0.060$. The data obtained with 290 nm excitation have been scaled and offset for comparison.

that the peptide undergoes a conformational change upon association with the vesicle, which shortens the separation distance between Trp and Phe_{CN}. Consequently, this leads to a more efficient fluorescence resonance energy transfer from the donor to the acceptor. Therefore, this result is consistent with the CD data obtained in the vesicle solution and corroborates the idea that the vesicle-bound magainin-2-P1 adopts a helical structure because the separation distance between Phe_{CN} and Trp in this case would be approximately 13 Å, slightly shorter than the Förster distance of this FRET pair. At such a separation distance, it is estimated that greater than 60% of the Phe_{CN} fluorescence would be quenched by the Trp via the mechanism of FRET. While the current fluorescence and CD results are useful in probing the equilibrium conformation of the vesicle-bound peptides, they do not provide direct information on the position and orientation of these peptides with respect to the membrane bilayer. However, for magainin-2, Jo et al.³² have shown that the helices become deeply inserted into the interior of the membrane at a peptide-to-lipid ratio similar to the value used in the current experiments.

Stopped-Flow Kinetics. The peptide–membrane association kinetics were obtained using a SFM-300 stopped-flow unit from Bio-logic (Claix, France) in conjunction with home-built optics. The mixing dead time of the current setup was ~1 ms, as characterized by the method detailed above. First, the peptide–vesicle association kinetics were probed by Trp fluorescence via direct excitation of the indole chromophore (i.e., $\lambda_{\text{ex}} = 290$ nm). As shown (Figure 4), the resultant stopped-flow trace shows two distinct phases with roughly the same amplitude, indicating that the association reaction proceeds through the formation of a kinetic intermediate. Similar results have also been observed in studies involving other peptides.^{18,37} For example, using stopped-flow Trp fluorescence Constantinescu et al.¹⁸ have shown that the association kinetics of melittin with POPC/POPG vesicles are biphasic. The two kinetic components are well separated in time but have rather similar amplitudes.

On the basis of studies where the lipid composition was varied or where fluorescein–phosphatidylethanolamine (FPE)-labeled lipids were used, the fast phase has been attributed to the process

of binding, whereas the slow phase was assigned to the process of peptide insertion.^{18,24,25} While these types of experiments allow the determination of the rate constant of the individual steps associated with the peptide-vesicle association, it cannot explicitly determine where the helix folding occurs.

Second, the peptide-vesicle association kinetics were probed by Trp fluorescence via indirect excitation of the indole chromophore, i.e., via FRET. As shown (Figure 4), the stopped-flow kinetic profile obtained using an excitation wavelength of 240 nm, which selectively excites Phe_{CN}, also exhibits two distinct phases; however, the amplitude of the fast phase is distinctly larger (>80%) than that of the slow phase. A quantitative analysis further indicated that these stopped-flow kinetics, obtained via either directly or indirectly exciting the Trp fluorescence, can be globally fit by two biexponential functions that differ only in their relative amplitudes. The fast exponential component has a time constant of 11 ± 2 ms, while the slow exponential component has a time constant of 99 ± 15 ms. These rates are similar to those determined for other peptides, such as melittin.¹⁸ Most importantly, however, these results allow us to directly assign the fast component, or the initial binding process, to the coil-to-helix transition step because such a process would significantly shorten the separation distance between the Phe_{CN} and Trp residues and, thus, lead to an increase of the FRET efficiency and moreover the Trp fluorescence. As a result, the relative amplitude of the fast component in the stopped-flow Trp fluorescence kinetics is significantly increased when only the donor is excited. Finally, it is worth pointing out that the poorer signal-to-noise ratio for the stopped-flow trace obtained with an excitation wavelength of 290 nm, compared to that collected with an excitation wavelength of 240 nm, is due to the smaller absorbance of the peptide sample at this wavelength.

To further verify that the fast stopped-flow kinetic phase is associated with the initial binding process, as suggested by other studies,^{22,24} we performed an additional experiment wherein the concentration of the vesicle was decreased by one-half. Since the initial binding reaction between the peptide and the vesicle under the current conditions is pseudo-first-order with respect to the peptide, such a reduction in the vesicle concentration is expected to result in a decrease in the pseudo-first-order reaction rate constant by 50%. As shown (Figure 5), the time constant of the fast phase is indeed increased to 23 ± 4 ms, which is (within our experimental uncertainty) twice as long as that observed for the initial vesicle concentration (Figure 4). Therefore, this experiment confirms that the helix formation is concomitant with the initial peptide binding process and indicates that the membrane-mediated helix folding rate is much slower than the folding rate of alanine-based helical peptides in solution.³⁸ Likely, this could be attributed to the large entropic cost associated with the specific binding of the peptide with the lipids, which stabilizes the nascent helix, akin to the process of helical protein folding wherein the rate of tertiary structure formation is always slower than that of secondary structure formation.

The coil-to-helix transition dynamics of a peptide can also be followed by monitoring the change in the donor fluorescence upon membrane association. As shown (Figure 6), the stopped-flow trace obtained by using a UV band-pass filter centered at 299 nm with a bandwidth of 22 nm shows that the Phe_{CN} fluorescence intensity decreases exponentially with time. While the signal-to-noise ratios of these data are poor, due to the low throughput (15–30%) of the filter used, the decay time constant obtained from the best fitting is about 10 ± 2 ms, which closely

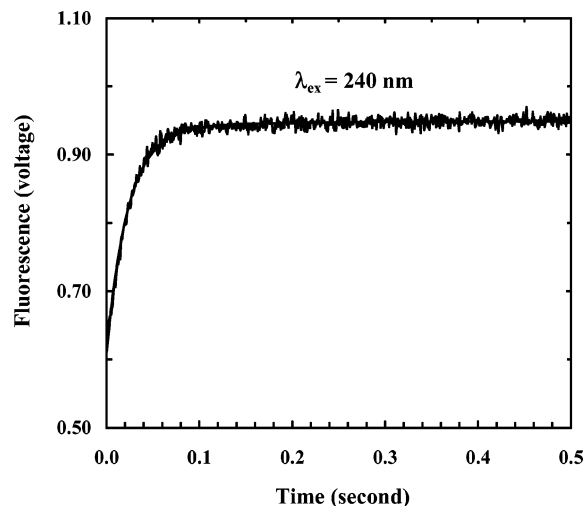


Figure 5. Stopped-flow fluorescence trace obtained with an excitation wavelength of 240 nm and a 315 nm long-pass filter. All other experimental conditions are the same as those used in Figure 4 except the vesicle concentration, which is one-half the original value. The smooth line corresponds to the fit to the following equation, $S(t) = A - B_1 \exp(-t/\tau_1) - B_2 \exp(-t/\tau_2)$, with $\tau_1 = 23$ ms, $\tau_2 = 99$ ms, $A = 0.949$, $B_1 = 0.324$, and $B_2 = 0.016$.

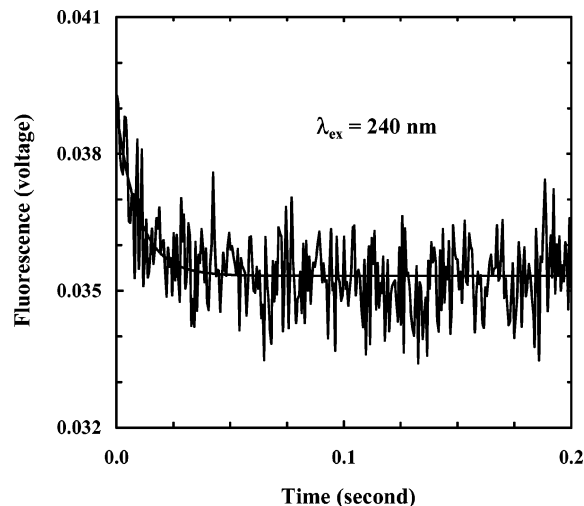


Figure 6. Stopped-flow fluorescence trace obtained using a UV band-pass filter centered at 299 nm. The smooth line is the fit to a single-exponential function with a time constant of 9.7 ms.

matches that observed in those experiments where the Trp fluorescence was used as the probe. Therefore, this result further corroborates the conclusions reached above. Taken together, these FRET experiments demonstrated the utility of using Phe_{CN} and Trp as a FRET pair, in conjunction with stopped-flow technique, to directly monitor the membrane-mediated helix folding dynamics.

Comparison to Existing Models. Several models have been proposed to describe the molecular mechanism of the peptide-membrane interaction.^{3,13–16,19,20,24,39–42} For example, Huang¹² and others^{13,14,43} have proposed that the peptide-membrane association follows a two-state model, or the SMH model.^{1,15–16,35} According to this model, the peptides, which are unfolded in the aqueous phase, first bind to the lipid/water interface and form α -helical structures. Then the helices insert into the interior of the lipid bilayers. Depending on peptide concentration and other conditions,³⁶ these bound peptides may further associate to form higher-order structures or remain as monomers. Because

of the relatively low peptide concentration used ($\sim 40 \mu\text{M}$), it is unlikely that peptide aggregates were formed in the current case.^{20,36}

Our stopped-flow FRET results clearly demonstrate that the folding of magainin-2-P1 occurs concomitantly with the initial binding of the peptide to the membrane and, therefore, are consistent with the notion that the peptide–membrane interaction follows a sequential, multistage mechanism wherein the secondary structure is quickly formed at or near the membrane surface.^{1,14} A stopped-flow CD study by Wang et al.²⁵ on the interaction of cecropin B with phospholipid vesicles containing 25% anionic lipid also showed that the helical structure is populated as a kinetic intermediate. Furthermore, despite using static methods (internal reflection infrared spectroscopy and Langmuir trough techniques), Silvestro and Axelsen⁴⁴ were able to isolate and study the intermediate stages of the interaction between cecropin A, a 37-residue membrane-active antimicrobial polypeptide, with a membrane. Their results indicated that cecropin A folds into an α -helical structure (with some β -structure) while superficially adsorbed to the membrane surface. Thus, they argued that the folding of cecropin A is driven by interactions with superficial components of the membrane, not deeper hydrophobic regions. Since magainin-2-P1 is found to fold at the early stage of its association with the membrane, similar arguments may also be applied to understand its folding.

The mechanism of peptide–membrane interaction has also been studied recently by various theoretical and simulation methods.^{13,17,19,45} For example, Im and Brooks¹⁷ and Garcia and co-workers¹⁹ have investigated the folding and binding behaviors of several predominantly hydrophobic peptides using a replica exchange molecular dynamics algorithm. The results of Im and Brooks,¹⁷ which suggest that the peptide first becomes localized at the membrane/solvent interface where it eventually forms significant helical secondary structure via a helix-turn-helix motif, seem to be in good agreement with our findings. While our result and also those of Im and Brooks suggest that the coil-to-helix transition occurs at the interfacial region of the membrane, further studies using peptides with different hydrophobicity and vesicles of different lipid composition are needed to confirm the generality of this mechanism. Additionally, stopped-flow studies on a series of peptides with different Phe_{CN}–Trp separation distances would help provide a better description of the helical conformations formed at the interfacial region.

Conclusion

In summary, we demonstrated that the Phe_{CN} and Trp FRET pair, in conjunction with the stopped-flow technique, can be used to directly monitor the coil-to-helix transition dynamics of membrane-binding peptides. While other methods have been developed to understand the structure, orientation, and thermodynamics of membrane-bound peptides,^{5–10,34,36} the current technique is uniquely poised to provide kinetic information that is difficult to be extracted by other means.

Acknowledgment. We gratefully acknowledge financial support from the National Institutes of Health (GM-065978 and RR-01348).

References and Notes

- (1) Zasloff, M. *Nature* **2002**, *415*, 389.
- (2) Rinaldi, A. C. *Curr. Opin. Chem. Biol.* **2002**, *6*, 799.
- (3) Epand, R. M.; Vogel, H. J. *Biochim. Biophys. Acta* **1999**, *1462*, 11.
- (4) Jacobs, R. E.; White, S. H. *Biochemistry* **1989**, *28*, 3421.
- (5) Bechinger, B.; Rysschaert, J. M.; Goormaghtigh, E. *Biophys. J.* **1999**, *76*, 552.
- (6) Wieprecht, T.; Apostolov, O.; Beyermann, M.; Seelig, J. *J. Mol. Biol.* **1999**, *294*, 785.
- (7) Ladokhin, A. S.; White, S. H. *Biochemistry* **2004**, *43*, 5782.
- (8) Tatulian, S. A.; Qin, S.; Pande, A. H.; He, X. *J. Mol. Biol.* **2005**, *351*, 939.
- (9) Bechinger, B.; Zasloff, M.; Opella, S. J. *Protein Sci.* **1993**, *2*, 2077.
- (10) Tucker, M. J.; Getahun, Z.; Nanda, V.; DeGrado, W. F.; Gai, F. *J. Am. Chem. Soc.* **2004**, *126*, 5078.
- (11) Mukherjee, P.; Krummel, A. T.; Fulmer, E. C.; Kass, I.; Arkin, I. T.; Zanni, M. T. *J. Chem. Phys.* **2004**, *120*, 10224.
- (12) Huang, H. W. *Biochemistry* **2000**, *39*, 8347.
- (13) Maddox, M. W.; Longo, M. L. *Biophys. J.* **2002**, *82*, 244.
- (14) Kandasamy, S. K.; Larson, R. G. *Chem. Phys. Lipids* **2004**, *132*, 113.
- (15) Matsuzaki, K. *Biochim. Biophys. Acta* **1999**, *1462*, 1.
- (16) Shai, Y. *Biochim. Biophys. Acta* **1999**, *1462*, 55.
- (17) Im, W.; Brooks, C. L. *Proc. Natl. Acad. Sci. U.S.A.* **2005**, *102*, 6771.
- (18) Constantinescu, I.; Lafleur, M. *Biochim. Biophys. Acta* **2004**, *1676*, 26.
- (19) Nymeyer, H.; Woolf, T. B.; Garcia, A. E. *Proteins* **2005**, *59*, 783.
- (20) Matsuzaki, K.; Murase, O.; Miyajima, K. *Biochemistry* **1995**, *34*, 12553.
- (21) Matsuzaki, K.; Yoneyama, S.; Murase, O.; Miyajima, K. *Biochemistry* **1996**, *35*, 8450.
- (22) Polozov, I. V.; Polozova, A. I.; Mishra, V. K.; Anantharamaiah, G. M.; Segrest, J. P.; Epand, R. M. *Biochim. Biophys. Acta* **1998**, *1368*, 343.
- (23) Pokorny, A.; Birkbeck, T. H.; Almeida, P. F. F. *Biochemistry* **2002**, *41*, 11044.
- (24) Golding, C.; Senior, S.; Wilson, M. T.; O'Shea, P. *Biochemistry* **1996**, *35*, 10931.
- (25) Wang, W.; Smith, D. K.; Moulding, K.; Chen, H. M. *J. Biol. Chem.* **1998**, *273*, 27438.
- (26) Roder, H.; Maki, K.; Cheng, H.; Shasthya, R. *Methods* **2004**, *34*, 15.
- (27) Haas, E.; Wilchek, M.; Katchalski-Katzir, E.; Steinberg, I. Z. *Proc. Natl. Acad. Sci. U.S.A.* **1975**, *72*, 1807.
- (28) Morgan, M. A.; Okamoto, K.; Kahn, J. D.; English, D. S. *Biophys. J.* **2005**, *89*, 2588.
- (29) Tucker, M. J.; Oyola, R.; Gai, F. *J. Phys. Chem. B* **2005**, *109*, 4788.
- (30) Du, D.; Tucker, M. J.; Gai, F. *Biochemistry* **2006**, *45*, 2668.
- (31) Williams, R. W.; Starman, R.; Taylor, K. M. P.; Gable, K.; Beeler, T.; Zasloff, M.; Covell, D. *Biochemistry* **1990**, *29*, 4490.
- (32) Jo, E.; Blazyk, J.; Boggs, J. M. *Biochemistry* **1998**, *37*, 13791.
- (33) Zhao, H.; Mattila, J. P.; Holopainen, J. M.; Kinnunen, P. K. *J. Biophys. J.* **2001**, *81*, 2979.
- (34) Wakamatsu, K.; Takeda, A.; Tachi, T.; Matsuzaki, K. *Biopolymers* **2002**, *64*, 314.
- (35) Yang, L.; Weiss, T. M.; Lehrer, R. I.; Huang, H. W. *Biophys. J.* **2000**, *79*, 2002.
- (36) Matsuzaki, K.; Murase, O.; Tokuda, H.; Funakoshi, S.; Fujii, N.; Miyajima, K. *Biochemistry* **1994**, *33*, 3342.
- (37) Bryson, E. A.; Rankin, S. E.; Carey, M.; Watts, A.; Pinheiro, T. J. *Biochemistry* **1999**, *38*, 9758.
- (38) Wang, T.; Zhu, Y.; Getahun, Z.; Du, D.; Huang, C.-Y.; DeGrado, W. F.; Gai, F. *J. Phys. Chem. B* **2004**, *108*, 15301.
- (39) Ludtke, S. J.; He, K.; Wu, Y.; Huang, H. W. *Biochim. Biophys. Acta* **1994**, *1190*, 181.
- (40) Milik, M.; Skolnick, J. *Proc. Natl. Acad. Sci. U.S.A.* **1992**, *89*, 9391.
- (41) Orlandini, E.; Seno, F.; Banavar, J. R.; Laio, A.; Maritan, A. *Proc. Natl. Acad. Sci. U.S.A.* **2000**, *97*, 14229.
- (42) Engelman, D. M.; Steitz, T. A. *Cell* **1981**, *23*, 411.
- (43) White, S. H.; Wimley, W. C. *Biochim. Biophys. Acta* **1998**, *1376*, 339.
- (44) Silvestro, L.; Axelsen, P. H. *Biophys. J.* **2000**, *79*, 1465.
- (45) Lopez, C. F.; Nielsen, S. O.; Moore, P. B.; Klein, M. L. *Proc. Natl. Acad. Sci. U.S.A.* **1991**, *101*, 4431–4434.